

# In-situ embedded stress sensing for additively manufactured multi-material ceramics via piezospectroscopy

Nicholas Reed<sup>a</sup>, Rishikesh Srinivasaraghavan Govindarajan<sup>a</sup>, Zachary Stein<sup>a</sup>, Seetha Raghavan<sup>a</sup>,  
Daewon Kim<sup>\*a</sup>

<sup>a</sup>Department of Aerospace Engineering, Embry-Riddle Aeronautical University, Daytona Beach, FL  
32114, United States

## ABSTRACT

Additive manufacturing (AM) has shown great potential for producing complex and highly customizable ceramic structures, especially when utilizing high resolution techniques such as vat photopolymerization. By leveraging recent advancements in fabricating multi-material ceramic structures, embedded sensing can be achieved with little to no additional post-processing of the fabricated part. This work demonstrates non-contact strain sensing capabilities of AM ceramic structures via photoluminescent piezospectroscopy. A ceramic substrate is fabricated via multi-material vat photopolymerization with an embedded  $\alpha$ -Al<sub>2</sub>O<sub>3</sub> (alumina) inclusion. The complex ceramic structure is characterized in compression, while examining the impact of the  $\alpha$ -Al<sub>2</sub>O<sub>3</sub> sensing inclusion on the structure's properties. The strain conditions of the structure and the inclusions undergoing deformation are monitored with digital image correlation (DIC). The sharp photoluminescent peaks obtained from the inclusion are then monitored for peak shifts to evaluate the strain condition of the structure under deformation, and compared with the DIC findings. By utilizing photoluminescent piezospectroscopy (PLPS) for in-situ damage detection, structures can be monitored immediately after, and even during, fabrication for irregularities and defects. Furthermore, by integrating non-contact sensing inclusions directly into the ceramic substrate, this work minimizes the need for external wiring channels and post-processing, significantly reducing the complexity of sensor integration into ceramic parts and increasing the lifetime of the structure.

**Keywords:** Additive Manufacturing, Embedded Sensing, Piezospectroscopy, In-Situ Stress Sensing, Non-Contact Sensing

## 1. INTRODUCTION

Advanced ceramics have been utilized in aerospace applications due to their exceptional thermal stability, mechanical strength, and chemical resistance. Traditional manufacturing of complex ceramic structures, especially ceramics enhanced with embedded sensors, is often challenging or even impossible with traditional manufacturing techniques. However, Additive Manufacturing (AM) has revolutionized the field of Structural Health Monitoring (SHM) by enabling the production of complex, intricately designed structures that were previously unattainable through conventional fabrication methods<sup>1-4</sup>. These structures can be enhanced to include embedded sensing, providing functionality previously not possible without these advances.

Vat photopolymerization, a process traditionally associated with polymer-based AM, is frequently utilized with ceramic-doped resins, which can be post-processed to produce fully ceramic parts<sup>5-6</sup>. The structures fabricated using this technique can be designed and manufactured with a high resolution, often on the order of microns, while maintaining a large overall structural size that can be up to cubic centimeters in volume<sup>7-8</sup>. Thus, using vat photopolymerization offers a unique combination of precision and ease of manufacture that other AM processes, such as FDM, often cannot offer.

Since this AM process utilizes liquid resin slurries to print parts, specialized vat photopolymerization printers can be used to fabricate unique multimaterial ceramic parts that are too challenging for traditional techniques to produce<sup>9-10</sup>. Specifically, multimaterial ceramic parts can be produced by changing the resin used during the 3D printing process, leading to ceramic green body parts that, when sintered, create seamless transitions between two different ceramics. By utilizing this technique, sensing capabilities can be easily embedded into a structure.

---

\* kimd3c@erau.edu; phone 386-226-7262; ERAU SMART Lab

One of the ways to utilize ceramics in embedded sensing involves applying photoluminescent piezospectroscopy (PLPS). PLPS is a technique for stress sensing in certain materials, specifically those with photoluminescent properties, such as alumina. When a photoluminescent material is excited with a suitable energy source, it produces a large spectral response<sup>11-13</sup>. Under mechanical load, the wavelength of this spectral response shifts, which can then be correlated to the applied loading. This technique is particularly useful for passive, non-contact, high-resolution stress sensing in structures where additional complex structures or materials cannot be embedded. Comparable techniques often require wiring or fiber optics to be embedded inside of the structure, which can cause structural variability due to the large material mismatch<sup>14-15</sup>. Additionally, wireless sensing techniques often require an internal power supply that must be recharged or replaced after a certain period of time<sup>16</sup>.

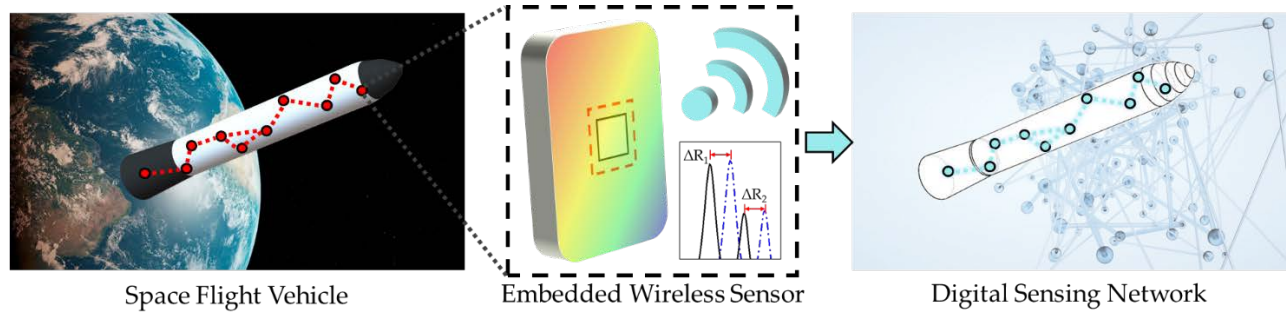


Figure 1. Embedded wireless sensor systems in action. A critical ceramic structure can be enhanced with embedded wireless sensors that enable the creation of a complex digital sensing network that can be utilized in harsh environmental conditions.

In this work, we leverage a state-of-the-art vat photopolymerization 3D printer to manufacture a complex multimaterial AM ceramic substrate, employing the PLPS sensing technique to produce a fully passive, wireless embedded stress sensor. This combination of cutting-edge AM technology with a unique sensing technique presents a novel advancement in SHM embedded sensing. The ability to create multimaterial ceramic components with seamless transitions enhances the versatility of these structures. Notably, it enables the use of techniques previously limited to certain materials and applications to a much broader scope of aerospace applications, as demonstrated in Figure 1.

## 2. MATERIALS AND FABRICATION

To demonstrate the sensing capabilities of the multimaterial ceramic structures, a series of experiments were performed, using the Lithoz 2M30 multimaterial ceramic printer to fabricate ceramic structures with embedded sensing regions. The 2M30 contains two separate and interchangeable vats that allow for up to two different materials to be printed in the same part with no restrictions on their orientation or layout. A wiper system cleans the parts between material changes to reduce cross contamination. As seen in Figure 2, the part was designed and printed as a 4 mm × 4 mm × 10mm rectangular block; after sintering this reduced the part size down to 3.4 mm × 3.1 mm × 8 mm. LithaLox 350, an  $\alpha$ -Al<sub>2</sub>O<sub>3</sub> (alumina) resin developed by Lithoz, was utilized for the embedded sensor. The substrate is made of LithaCon 3Y 210, another commercial resin developed by Lithoz, primarily composed of Yttria Stabilized Zirconia (YSZ). These materials do not have greatly different shrinkage ratios during sintering, making them relatively compatible with each other. The printing parameters used are given below in Table 1:

Table 1. Printing parameters for the Lithoz 2M30 printer during fabrication of the multimaterial ceramic samples.

	YSZ	Alumina
Layer Height	50 $\mu$ m	
Tilt Up Speed	8 $^{\circ}$ /s	
Tilt Down Speed	4 $^{\circ}$ /s	
DLP Energy	180 mJ/cm <sup>2</sup>	250 mJ/cm <sup>2</sup>
DLP Intensity	50 mW/cm <sup>2</sup>	
Settling Time	10 s	

After the completion of the printing process, the fabricated samples were cleaned, dried, and sintered. LithaSol 20 (Lithoz's proprietary solvent) was used to clean the parts of excess slurry. Once dry, the parts underwent a two-step sintering process, as shown in Figure 3.

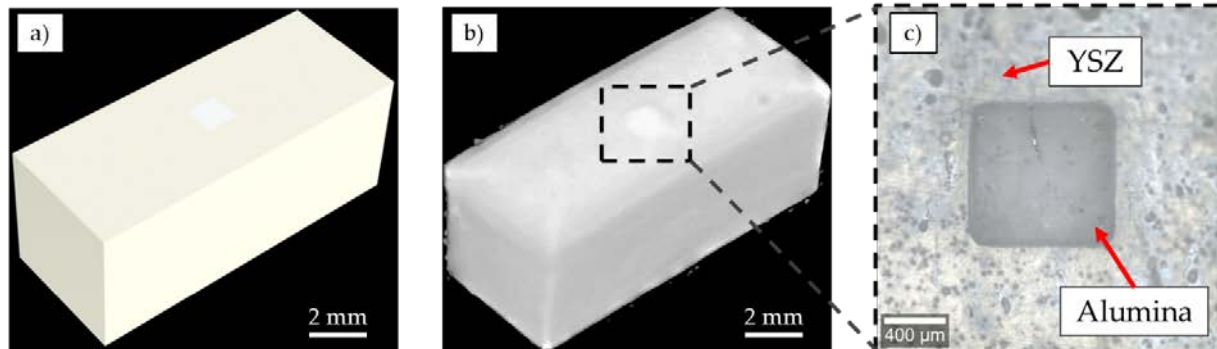


Figure 2. The a) designed and b) manufactured compression sensor sample. c) A top view of the alumina insert that was embedded into the surface of the YSZ compression block. Good bonding is seen between the YSZ and alumina was observed.

For the debinding process, a series of small ramps and holds are performed before a large ramp to 1150 °C at a rate of 1 °C/min, followed by controlled cooling. Afterwards, the ceramic samples are slowly ramped to 1450 °C at a max rate of 1.5 °C/min, where they are held at temperature for 960 minutes, followed by another controlled cooling. After sintering, the sample was painted with a DIC speckle on the side.

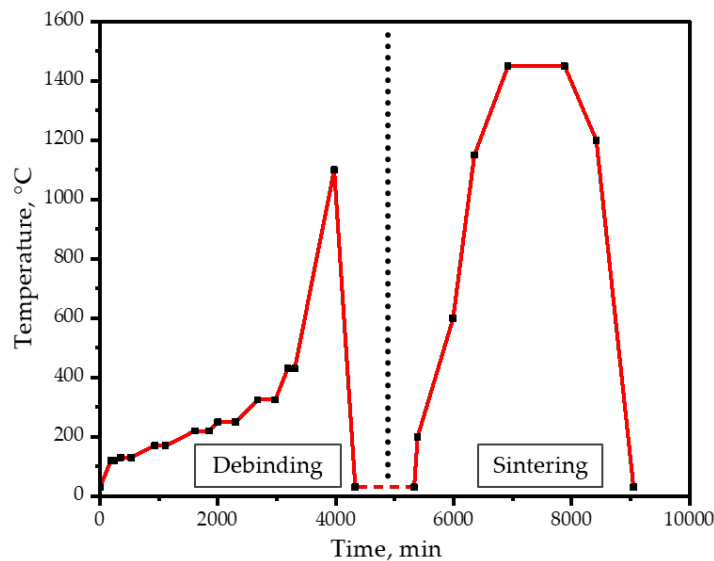


Figure 3. The sintering firing schedule for the ceramic samples. The process is split into two separate sections, one for removal of polymer, and another for densification of the ceramics.

### 3. EXPERIMENTAL DESIGN

After fabricating the samples, they were tested in-situ with a Psylotech load frame. The samples were compressed to 1200 N, at 6 even loading intervals of 200 N. During the load process at each loading step, photoluminescent (PL) scans were acquired with a WITec Confocal Raman microscope, as shown in Figure 4. The curves were acquired at 10 mW excitation source with a 0.05 s integration time, a 532 nm laser excitation source, and a 10x microscope objective. After the PL peaks were gathered, they were peak-fitted with a Lorentzian fit to obtain the peak position at the loading interval<sup>17</sup>. These peaks are then analyzed to determine the overall peak shift. A VIC-3D DIC system was used to track the strains from the compressed samples.

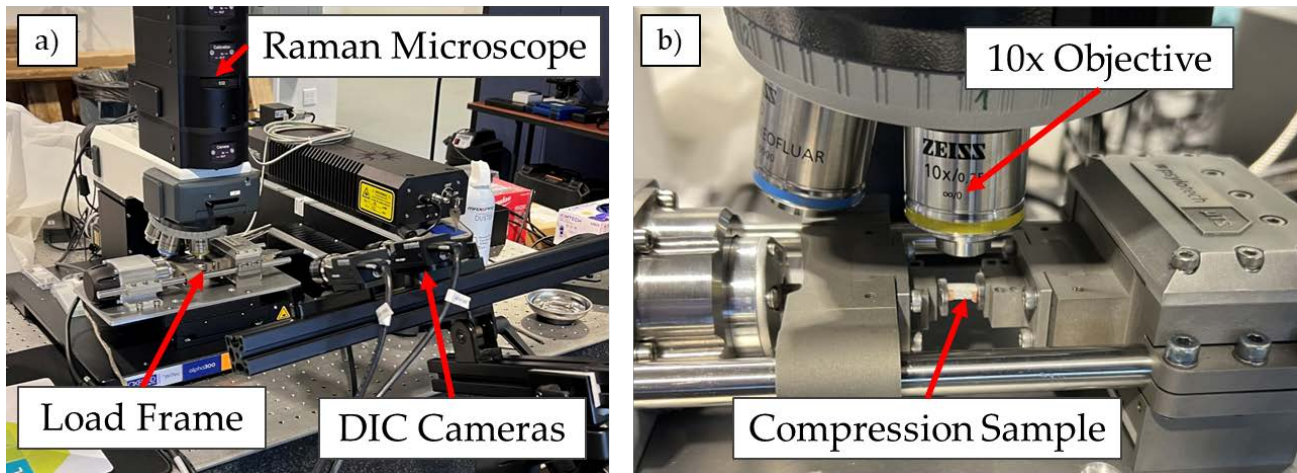


Figure 4. The experimental setup for the integrated experiments. The sensor sample was loaded in the Psylotech load frame, along with sapphire compression platens. The load frame and sample were then attached to a moving stage underneath the WITec Raman confocal microscope, which allowed for photoluminescence scans during the loading process. DIC cameras were positioned to observe the side of the sensor sample, which is painted with a speckle pattern to track the displacements in the compression sample.

Additionally, hardness measurements were taken to verify the structural integrity of the ceramic samples post-sintering. A Wilson Tukon 1202 Micro Hardness tester (Lake Bluff, IL, USA) was used to apply load to sintered ceramic samples using a Vickers microindenter. A load of 1 kgf was applied at each testing point. The hardness value was derived from the indentation diagonal length, according to ASTM C1327-19<sup>18</sup>, with the indent lengths verified with microscopy and all low-quality indents removed.

## 4. RESULTS AND DISCUSSION

### 4.1 Hardness Validation

The results of the hardness testing are shown in Table 2. The YSZ showed a hardness value of 1263 HV, while the alumina showed a hardness of 1538 HV. These values strongly match the manufacturer's specifications for the solid bulk material (1250 HV and 1550 HV, respectively), indicating that the manufacturing process was sufficient to fully densify the ceramic and produce functional multimerial ceramic parts.

Table 2. Results of the Vickers hardness testing.

Material	YSZ	Alumina
Hardness Value (HV)	1263.16	1538.45
Confidence Interval	112.15	78.47

### 4.2 PLPS Stress Sensing Validation

The PLPS data showed a strong linear correlation with increasing load, as shown in Figure 5. As seen in Table 3, the spectral shifts observed at each loading interval indicated an average stress coefficient of 5.45  $\text{cm}^{-1}/\text{GPa}$  for the  $R_1$  peak, and 5.85  $\text{cm}^{-1}/\text{GPa}$  for the  $R_2$  peak. These coefficients are larger than the theoretical values for alumina under compression<sup>19</sup>, however, the loading experienced by the polycrystalline embedded sensing element is mechanically more complex than uniaxial compression, causing an increase in the spectroscopic coefficients. The peaks show strong linearity, even for lower loading conditions, which can be challenging for pure alumina ceramic PLPS. Both peaks are viable for stress sensing, with minor differences between them. Additionally, the responses from the embedded ceramic insert were very strong, even at very low power and integration time, indicating that the data acquisition range of the sensor can be greatly extended beyond a close-range scan<sup>20</sup>.

Table 3. Results of the PLPS testing.

	R <sub>1</sub> Coefficient (cm <sup>-1</sup> /GPa)	R <sub>1</sub> Linear Fit (R <sup>2</sup> )	R <sub>2</sub> Coefficient (cm <sup>-1</sup> /GPa)	R <sub>2</sub> Linear Fit (R <sup>2</sup> )
Test 1	5.3	0.999	5.8	0.99
Test 2	5.6	0.994	5.9	0.994

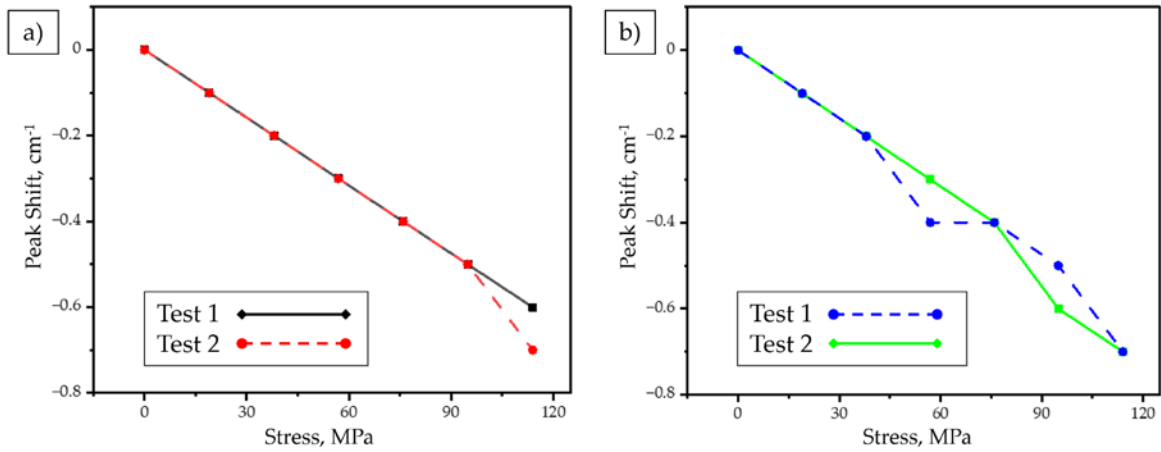


Figure 5. The results of the PLPS testing. Both the a) R1 and b) R2 peaks show strong linear peak shift, indicating good sensitivity to applied loading. Both peaks exhibit strong linearity as well, with little variation in the peak shift compared to the applied loading. The R2 peak features a slightly higher peak shift, while the R1 peak provides a slightly more consistent response.

### 4.3 DIC Strain Validation

The results of the DIC testing are shown in Figure 6. The DIC shows a linear response from the ceramic material, indicating good structural stability in the fabricated sample, with little to no structural defects. The modulus of elasticity was found to be 155 GPa, slightly lower than the theoretical value for YSZ (200 GPa). However, due to the lower loading condition (max load of 115 MPa), as well as the multimaterial insert creating a change in modulus, this is a relatively good match with the theoretical value.

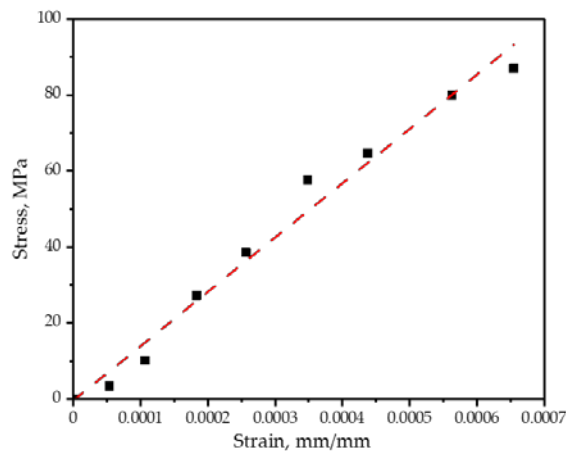


Figure 6. The results of the DIC from the tested sample. The DIC shows good linearity during the compressive loading of the sample and verifies a stress response consistent with that of a majority bulk YSZ material.

## 5. CONCLUSION

This work demonstrates the viability and efficacy of utilizing vat photopolymerization additive manufacturing to fabricate multimaterial ceramic structures with passive wireless embedded sensors. The integration of photoluminescent piezospectroscopy within these structures provides a reliable method for non-contact stress sensing, with the observed spectral shifts exhibiting strong linearity (minimum  $R^2$  of 0.99) with applied compressive loads. Furthermore, DIC analysis confirmed the structural integrity and mechanical stability of the fabricated samples, while hardness measurements indicated material properties consistent with bulk materials. These results highlight the potential of advanced ceramic additive manufacturing in the development of effective sensing systems for structural health monitoring of aerospace structures. The ability to seamlessly integrate different ceramic materials within a single structure expands the scope of sensing technologies to new materials and applications, enabling the development of more robust and customizable aerospace components. Future research should explore the scalability of this approach and investigate additional ceramic material combinations to further enhance the functionality and adaptability of these advanced embedded sensors.

## ACKNOWLEDGEMENTS

This material is based upon work supported by the National Science Foundation under Grant No. 2229155. The opinions, findings, and conclusions, or recommendations expressed are those of author(s) and do not necessarily reflect the views of the National Science Foundation.

## REFERENCES

- [1] Srinivasaraghavan Govindarajan, R., Rojas-Nastrucci, E., & Kim, D. (2021). Surface acoustic wave-based flexible piezocomposite strain sensor. *Crystals*, 11(12), 1576. <https://doi.org/10.3390/cryst11121576>
- [2] Reed, N., & Kim, D. (2022, September). Development of embeddable additive manufacturing microsensors for structural health monitoring. In *Smart Materials, Adaptive Structures and Intelligent Systems* (Vol. 86274, p. V001T05A006). American Society of Mechanical Engineers. <https://doi.org/10.1115/SMASIS2022-91047>
- [3] Sikulskyi, S., Govindarajan, R. S., Stark, T., Ren, Z., Reed, N., & Kim, D. (2024). Two-photon polymerized wetting morphologies for tunable external and internal electrode micropatterning. *Additive Manufacturing*, 86, 104220. <https://doi.org/10.1016/j.addma.2024.104220>
- [4] Hassani, S., & Dackermann, U. (2023). A systematic review of advanced sensor technologies for non-destructive testing and structural health monitoring. *Sensors*, 23(4), 2204. <https://doi.org/10.3390/s23042204>
- [5] Reed, N., Srinivasaraghavan Govindarajan, R., Perry, S., Coote, K., & Kim, D. (2024). Development of Additively Manufactured Embedded Ceramic Temperature Sensors via Vat Photopolymerization. *Crystals*, 14(11), 936. <https://doi.org/10.3390/cryst14110936>
- [6] Dadkhah, M., Tulliani, J. M., Saboori, A., & Iuliano, L. (2023). Additive manufacturing of ceramics: Advances, challenges, and outlook. *Journal of the European Ceramic Society*, 43(15), 6635-6664. <https://doi.org/10.1016/j.jeurceramsoc.2023.07.033>
- [7] Chen, Z., Li, Z., Li, J., Liu, C., Lao, C., Fu, Y., ... & He, Y. (2019). 3D printing of ceramics: A review. *Journal of the European Ceramic Society*, 39(4), 661-687. <https://doi.org/10.1016/j.jeurceramsoc.2018.11.013>
- [8] Srinivasaraghavan Govindarajan, R., Ren, Z., Melendez, I., Boetcher, S. K., Madiyar, F., & Kim, D. (2024). Polymer nanocomposite sensors with improved piezoelectric properties through additive manufacturing. *Sensors*, 24(9), 2694. <https://doi.org/10.3390/s24092694>
- [9] Bandyopadhyay, A., & Heer, B. (2018). Additive manufacturing of multi-material structures. *Materials Science and Engineering: R: Reports*, 129, 1-16. <https://doi.org/10.1016/j.mser.2018.04.001>
- [10] Chen, H., Guo, L., Zhu, W., & Li, C. (2022). Recent advances in multi-material 3D printing of functional ceramic devices. *Polymers*, 14(21), 4635. <https://doi.org/10.3390/polym14214635>
- [11] Freihofer, G., Schülzgen, A., & Raghavan, S. (2014). Multiscale mechanics to determine nanocomposite elastic properties with piezospectroscopy. *Acta materialia*, 81, 211-218. <https://doi.org/10.1016/j.actamat.2014.08.003>
- [12] Fouliard, Q., Ghosh, R., & Raghavan, S. (2020). Quantifying thermal barrier coating delamination through luminescence modeling. *Surface and Coatings Technology*, 399, 126153. <https://doi.org/10.1016/j.surfcoat.2020.126153>

- [13] Hanhan, I., Selimov, A., Carolan, D., Taylor, A. C., & Raghavan, S. (2017). Quantifying alumina nanoparticle dispersion in hybrid carbon fiber composites using photoluminescent spectroscopy. *Applied spectroscopy*, 71(2), 258-266. <https://doi.org/10.1177/0003702816662623>
- [14] Ghazanfari, A., Li, W., Leu, M. C., Zhuang, Y., & Huang, J. (2016). Advanced ceramic components with embedded sapphire optical fiber sensors for high temperature applications. *Materials & Design*, 112, 197-206. <https://doi.org/10.1016/j.matdes.2016.09.074>
- [15] Petrie, C. M., Leonard, D. N., Yang, Y., Trammell, M. P., Jolly, B. C., & Terrani, K. A. (2019). Embedment of sensors in ceramic structures (No. ORNL/SPR-2019/1301). Oak Ridge National Laboratory (ORNL), Oak Ridge, TN (United States). <https://doi.org/10.2172/1564172>
- [16] Providakis, C. P., Liarakos, E. V., & Kampianakis, E. (2013). Nondestructive Wireless Monitoring of Early-Age Concrete Strength Gain Using an Innovative Electromechanical Impedance Sensing System. *Smart Materials Research*, 2013(1), 932568. <https://doi.org/10.1155/2013/932568>
- [17] Lu, N., Zhang, Y., & Qiu, W. (2021). Comparison and selection of data processing methods for the application of Cr<sup>3+</sup> photoluminescence piezospectroscopy to thermal barrier coatings. *Coatings*, 11(2), 181. <https://doi.org/10.3390/coatings11020181>
- [18] ASTM C1327-19; Standard Test Method for Vickers Indentation Hardness of Advanced Ceramics. ASTM International: West Conshohocken, PA, USA, 2014.
- [19] He, J., & Clarke, D. R. (1995). Determination of the piezospectroscopic coefficients for chromium-doped sapphire. *Journal of the American Ceramic Society*, 78(5), 1347-1353. <https://doi.org/10.1111/j.1151-2916.1995.tb08493.x>
- [20] Frehofer, G., Dustin, J., Tat, H., Schülzgen, A., & Raghavan, S. (2015). Stress and structural damage sensing piezospectroscopic coatings validated with digital image correlation. *Aip Advances*, 5(3). <https://doi.org/10.1063/1.4916760>